

## 3-D reconstructions of the early-November 2004 CDAW geomagnetic storms: analysis of Ooty IPS speed and density data

M. M. Bisi<sup>1</sup>, B. V. Jackson<sup>1</sup>, J. M. Clover<sup>1</sup>, P. K. Manoharan<sup>2</sup>, M. Tokumaru<sup>3</sup>, P. P. Hick<sup>1,4</sup>, and A. Buffington<sup>1</sup>

<sup>1</sup>Center for Astrophysics and Space Sciences, University of California, San Diego, 9500 Gilman Drive #0424, La Jolla, CA 92093-0424, USA

<sup>2</sup>Radio Astronomy Centre, National Centre for Radio Astrophysics, Tata Institute of Fundamental Research, Udhagamandalam (Ooty), 643 001, India

<sup>3</sup>Solar-Terrestrial Environment Laboratory (STELab), Nagoya University, Furo-cho, Chikusa-ku, Nagoya 464-8601, Japan

<sup>4</sup>San Diego Supercomputer Center, University of California, San Diego, 9500 Gilman Drive #0505, La Jolla, CA 92093-0505, USA

Received: 13 June 2009 – Revised: 16 October 2009 – Accepted: 25 November 2009 – Published: 10 December 2009

**Abstract.** Interplanetary scintillation (IPS) remote-sensing observations provide a view of the solar wind covering a wide range of heliographic latitudes and heliocentric distances from the Sun between  $\sim 0.1$  AU and 3.0 AU. Such observations are used to study the development of solar coronal transients and the solar wind while propagating out through interplanetary space. They can also be used to measure the inner-heliospheric response to the passage of coronal mass ejections (CMEs) and co-rotating heliospheric structures. IPS observations can, in general, provide a speed estimate of the heliospheric material crossing the observing line of site; some radio antennas/arrays can also provide a radio scintillation level. We use a three-dimensional (3-D) reconstruction technique which obtains perspective views from outward-flowing solar wind and co-rotating structure as observed from Earth by iteratively fitting a kinematic solar wind model to these data. Using this 3-D modelling technique, we are able to reconstruct the velocity and density of CMEs as they travel through interplanetary space. For the time-dependent model used here with IPS data taken from the Ootacamund (Ooty) Radio Telescope (ORT) in India, the digital resolution of the tomography is  $10^\circ$  by  $10^\circ$  in both latitude and longitude with a half-day time cadence. Typically however, the resolutions range from  $10^\circ$  to  $20^\circ$  in latitude and longitude, with a half- to one-day time cadence for IPS data dependant upon how much data are used as input to the tomography. We compare reconstructed structures during early-November 2004 with in-situ measurements from the Wind spacecraft orbiting the Sun-Earth  $L_1$ -Point to val-

idate the 3-D tomographic reconstruction results and comment on how these improve upon prior reconstructions.

**Keywords.** Interplanetary physics (General or miscellaneous) – Radio science (Remote sensing) – Solar physics, astrophysics, and astronomy (Flares and mass ejections)

### 1 Introduction

This paper uses interplanetary scintillation (IPS) data from the Ootacamund (Ooty) Radio Telescope (ORT) (e.g., Swarup et al., 1971; Manoharan et al., 2000, 2001) taken during October/November 2004 (Carrington rotation 2022.5–2023.5) from observations at 327 MHz, and compares these with in-situ measurements from the Wind – Solar Wind Experiment (Wind|SWE) (Ogilvie and Desch, 1997; Ogilvie et al., 1995). These comparisons use three-dimensional (3-D) reconstructions (e.g., Jackson and Hick, 2005), similar to Bisi et al. (2008a) using Solar-Terrestrial Environment Laboratory (STELab) IPS observations and Solar Mass Ejection Imager (SMEI) white-light data for this same interval. A preliminary discussion of the Ooty data has been provided by Bisi et al. (2009c).

IPS observations of the solar wind, solar wind transients, and the inner-heliosphere, have been used for around 45 years (e.g., Hewish et al., 1964; Kojima and Kakinuma, 1990; Manoharan et al., 2000; Bisi, 2006; Jones et al., 2007; Bisi et al., 2009b). IPS is a powerful tool to probe the interplanetary medium. It is the rapid variation in signal received by radio antennas on Earth arising from the scattering of radio waves from a distant, compact, natural radio source passing through density inhomogeneities within the outwardly-propagating solar wind. IPS observations allow



Correspondence to: M. M. Bisi  
(mmbisi@ucsd.edu)

the solar wind speed to be inferred over all heliographic latitudes and a wide range of heliocentric distances (dependent upon observing frequency, the location of observable sources in the sky, and the radio source strength). For a single radio antenna (such as with Ooty) the outflow speed (IPS velocity) is determined from the power spectrum of the IPS observation, as described in detail by Manoharan and Ananthakrishnan (1990). These velocity determinations differ from those of multi-station IPS antennas since a cross-correlation analysis is used when simultaneous observations of the same radio source are obtained, see Jones et al. (2007) and references therein for a more-detailed explanation. Using a proxy of the scintillation-level converted to the disturbance factor level,  $g$ -level, the solar wind density can also be inferred from these IPS observations in the 3-D reconstructions (e.g., Hick and Jackson, 2004; Jackson and Hick, 2005; Breen et al., 2008). The 3-D velocity reconstructions can take place directly from the IPS velocity measurements however. The resulting reconstructions are of an inner-heliosphere region typically ranging from 15 solar radii out to approximately 3 astronomical units (AU).

The  $g$ -level is defined by Eq. (1).

$$g = m / \langle m \rangle \quad (1)$$

Here,  $m$  is the observed scintillation level, and  $\langle m \rangle$  is the mean level of scintillation for the source at its elongation at the time of the observation. Scintillation-level measurements from Ooty are available for each astronomical radio source as an intensity variation of signal strength (resulting from the small-scale variations in density,  $\Delta N_e$ ). Further discussion of determining  $g$ -level can be found in Jackson et al. (1998), and references therein.

The  $g$ -level proxy for density uses Eq. (2) since density values along the line of sight are not known a priori but are assumed for small-scale variations with a power-law scaling of heliospheric density.

$$\Delta N_e = A_c R^\alpha N_e^\beta \quad (2)$$

Here,  $A_c$  is a proportionality constant,  $R$  is the radial distance from the Sun,  $\alpha$  is a power of the radial falloff, and  $\beta$  is the power of the density.  $A_c$ ,  $\alpha$ , and  $\beta$  are determined using best-fit comparisons with in-situ measurements at 1 AU for 327 MHz observations. The values used here are as previously used for 327 MHz IPS observations:  $A_c$  is set equal to 1, and the two powers  $\alpha$  and  $\beta$ , are  $-3.5$  and  $0.7$ , respectively. Further detailed discussion can be found in Jackson et al. (2003) and references therein.

The 3-D tomographic reconstructions use perspective views of solar co-rotating plasma (Jackson et al., 1998) and of outward-flowing solar wind (Jackson and Hick, 2005) crossing the IPS observing lines of sight from Earth to the radio source. Both velocity and density are obtained through the use of a kinematic solar wind model. This model is

based on the conservation of mass and mass flux in the heliosphere as structure propagates outward with a radial assumption from a model-source-surface at  $15 R_\odot$  out to 3 AU. The IPS data are then fitted iteratively to refine this model over 18 iterations to guarantee convergence to a final best-fit solution. We then compare the resulting reconstructions with hourly-averaged in-situ measurements from Wind|SWE. Previous comparisons (Harra et al., 2007; Bisi et al., 2008a; Bisi et al., 2009c) have been with data from the Advanced Composition Explorer – Solar Wind Electron, Proton and Alpha Monitor (ACE|SWEPAM) (Stone et al., 1998; McComas et al., 1998) for this interval. Jackson and Hick (2005) describe the time-dependent 3-D tomographic technique in detail (first introduced in 2000).

The Ooty 3-D reconstruction used here in both velocity and density has a latitude and longitude digital resolution of  $10^\circ \times 10^\circ$  with 0.1 AU increments out from the model-source-surface. The half-day time cadence has 3-h interpolated increments, to yield output eight times a day for the modelled structure of the inner heliosphere. The outputs of such tomographic reconstructions using SMEI data have successfully provided a “source surface” input into the ENLIL 3-D magnetohydrodynamic (MHD) numerical model (e.g., Odstrcil and Pizzo, 2002). When propagated out through the interplanetary medium this compares equally as well with in-situ measurements (Bisi et al., 2008a).

Section 2 describes the observing interval. Section 3 outlines the Ooty 3-D velocity and density reconstructions. Section 4 holds discussion, and Sect. 5 provides conclusions.

## 2 Observations

October/November 2004 was a time of complex activity toward the end of the declining phase of Solar Cycle 23, with multiple CME features (which included several “Halo” and “Partial Halo” CMEs) as seen in images (Fig. 1) taken by the SOLar and Heliospheric Observatory – Large Angle Spectrometric COronagraph (SOHO|LASCO) (Domingo et al., 1995; Brueckner et al., 1995) C2 instrument and the SOHO – Extreme-Ultraviolet Imaging Telescope (SOHO|EIT) (Delaboudinière et al., 1995). The interplanetary counterparts (ICMEs) were also measured by space-borne in-situ plasma and magnetic-field instruments orbiting the Sun-Earth L<sub>1</sub>-Point. The time interval investigated here includes several ICMEs arising from the series of CMEs originating from the Sun between 4 November 2004 and 8 November 2004 (as first discussed by Harra et al., 2007), summarised in Table 1 here. During this time interval, two ICMEs with magnetic cloud (MC) characteristics occurred which had opposing magnetic orientations despite the fact that they were related to flares coming from above the same active region (AR) on the Sun. MCs are a subset of ICMEs which were first described by Burlaga (1995) as having strong magnetic fields (when compared with their surroundings) displaying

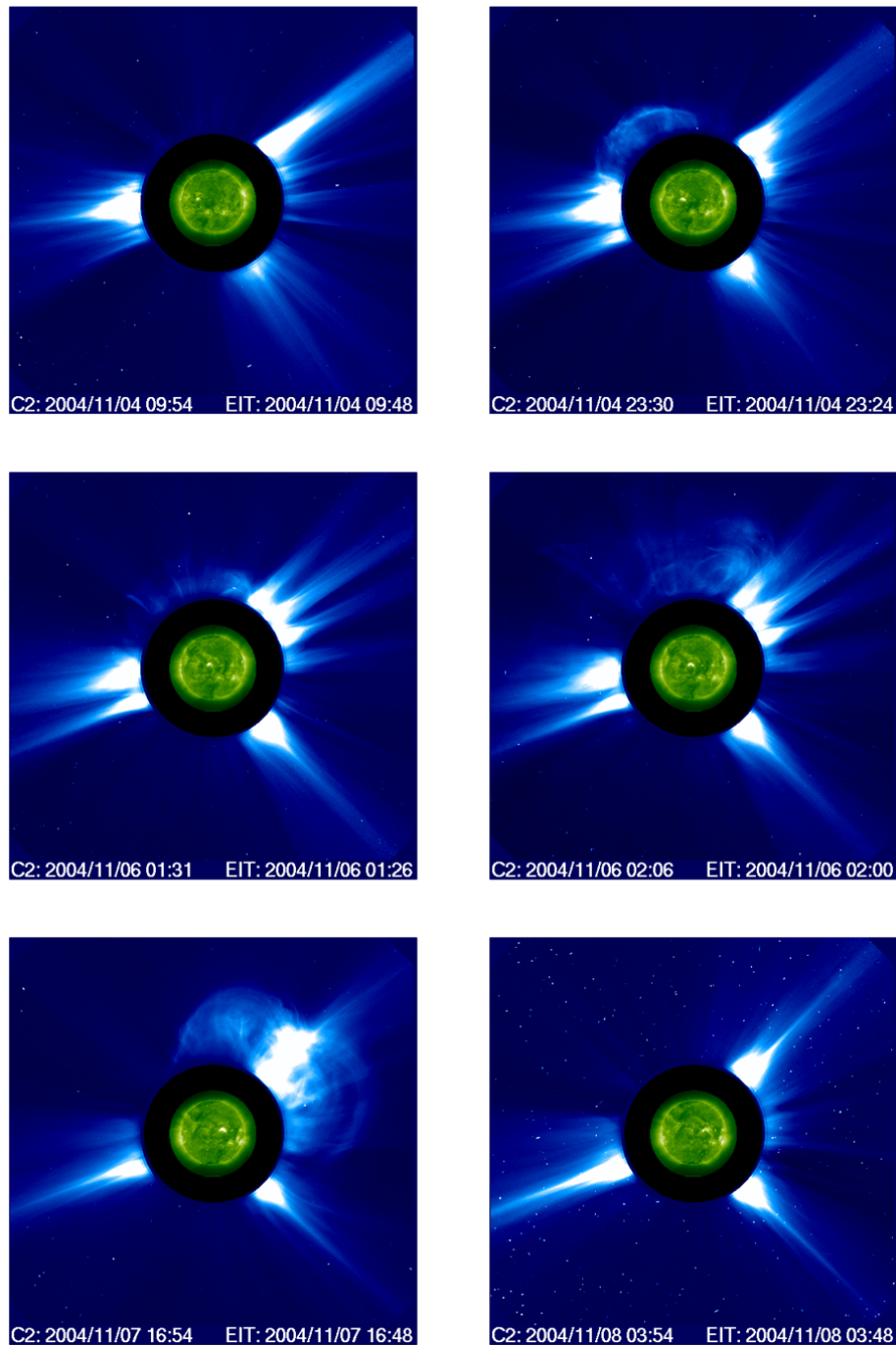


**Fig. 1.** Figure showing six composite images taken by the SOHO|LASCO C2 and SOHO|EIT instruments. The earlier five images are related to the events discussed here as summarised in Table 1. The sixth image (bottom right) is likely not related to the geomagnetic storms at the Earth (as described in the text) but may be visible in the reconstructed images (see later figures and respective explanations in the text). Images were taken from the Coordinated Data Analysis Workshop (CDAW) database ([http://cdaw.gsfc.nasa.gov/CME\\_list/](http://cdaw.gsfc.nasa.gov/CME_list/)) on the World Wide Web.

a large-and-coherent magnetic rotation, and a depressed ion temperature; thus, these were named as MCs. During these CME eruptions and resulting MCs, the AR's magnetic

configuration remained unchanged throughout (Harra et al., 2007).

**Table 1.** A summary of the events investigated here in chronological order of their possible source(s) as seen by the SOHO|LASCO C2 instrument. Table taken from Bisi et al. (2008a) and information partially taken from Zhang et al. (2007a) and also from Harra et al. (2007).

Possible LASCO C2 source (CME)	Interplanetary counterpart first seen at ACE	Geomagnetic activity ( $D_{st}$ minimum)
4 November 2004 – 09:54 UT Halo	7 November 2004 – 22:30 UT	8 November 2004 – 07:00 UT
4 November 2004 – 23:30 UT Partial Halo	7 November 2004 – 22:30 UT	8 November 2004 – 07:00 UT
6 November 2004 – 01:32 UT Halo	9 November 2004 – 20:25 UT	10 November 2004 – 10:00 UT
6 November 2004 – 02:06 UT Partial Halo	9 November 2004 – 20:25 UT	10 November 2004 – 10:00 UT
7 November 2004 – 16:54 UT Halo	9 November 2004 – 20:25 UT	10 November 2004 – 10:00 UT

The Living With a Star (LWS) Coordinated Data Analysis Workshop (CDAW) study conducted by Zhang et al. (2007a,b) also included these early-November 2004 events during their extensive analyses of large geoeffective storms with  $D_{st}$  (disturbance storm time index)  $\leq -100$  nT occurring between 1996 and 2005. Harra et al. (2007) cover the magnetic evolution of this time interval, and Bisi et al. (2008a) cover the 3-D STELab velocity and SMEI density analyses for this time interval. The Ooty 3-D analysis shown here improves upon the STELab and SMEI analyses when compared with in situ measurements, but the overall large-scale structures of velocity and density in the inner heliosphere are similarly reconstructed throughout this interval.

### 3 Ooty 3-D velocity and density reconstructions

Radio sources beyond  $11.5^\circ$  solar elongation (typically to  $\sim 60^\circ$  at 327 MHz, depending on the availability and strength of radio sources) were used in the velocity and density tomographic reconstructions using the kinematic solar wind model. Ooty IPS observations throughout this time interval covered a wide range of sources both to the North and to the South in the sky, as well as to the East and to the West of the Sun–Earth line. The Ooty telescope is capable of observing  $\sim 1000$  sources per day at its maximum, but for the interval concerned here, a total of 7248 observations of both velocity and  $g$ -level were used.

Here, the latitude and longitude spatial resolution is  $10^\circ$  with height increments of 0.1 AU out from the Sun, and a temporal cadence of a half day. This improved spatial and temporal resolution over previous STELab lower spatial and temporal resolution IPS 3-D reconstructions is due to the increased number of observations from the Ooty telescope throughout this time interval. The reconstructed parameters compare well with Wind in-situ measurements (also averaged over a half-day cadence) when using both the Ooty IPS velocity, and its scintillation-level converted to  $g$ -level value as a proxy for density. These in-situ comparisons can be seen in Fig. 2. Both the velocity and density are somewhat enhanced over those measured in situ, but the timing and general structure of the peaks correlate very well. Two features are marked on the plots: (A) The heliospheric struc-

ture associated with the front edge of the interplanetary disturbance which caused the 8 November 2004 geomagnetic storm (most likely caused by a combination of Earth-directed CMEs seen in LASCO C2 on 4 November 2004 at 09:54 UT and 23:30 UT); and (B) A combination of the 6 November 2004, 01:32 UT (halo) and 02:06 UT, LASCO C2 CMEs, consistent with the STELab IPS velocity and density reconstruction shown in Harra et al. (2007). Both are consistent with the SMEI (higher spatial resolution) density reconstruction shown in Bisi et al. (2008a) with some final material following behind resulting in a third peak in the in-situ data centred around 12 November 2004 (Fig. 2) likely a result of the later CME on 8 November 2004 (bottom-right image of Fig. 1) not related to the two geomagnetic storms of interest here.

### 4 Discussion

On 8 and 10 November 2004 at 07:00 UT and 10:00 UT respectively, the LWS CDAW storms (Zhang et al., 2007a,b) reached  $D_{st}$  minima at Earth. The interplanetary drivers of these storms are reconstructed (as seen in Figs. 3 and 4) in three dimensions and show what could be described as a “merging” of events in the inner heliosphere. The Ooty reconstruction results are consistent with those seen using STELab IPS and SMEI data in Bisi et al. (2008a). The signal-to-noise ratio (S/N) of Ooty is relatively high ( $S/N \geq 25$  for a 1 Jy radio source and a 1 s integration time). Each IPS observation should have smaller errors, which can be essential to reflect the actual state of the inner heliosphere. The Ooty results qualitatively show similarly-sized and similarly-shaped structures as those reconstructed from STELab and SMEI observations (as seen in Figs. 3 and 4). In addition, they quantitatively show a somewhat better match to the in-situ measurements obtained from the Wind spacecraft (as shown in Fig. 2). These interplanetary events led to the large geoeffective space-weather storms seen at Earth. What “merging” means here is likely the interaction of CMEs seen separately in white-light coronagraph data with the faster catching up with the slower, to form combined interplanetary counterparts. The Ooty 3-D analyses, Figs. 3 and 4

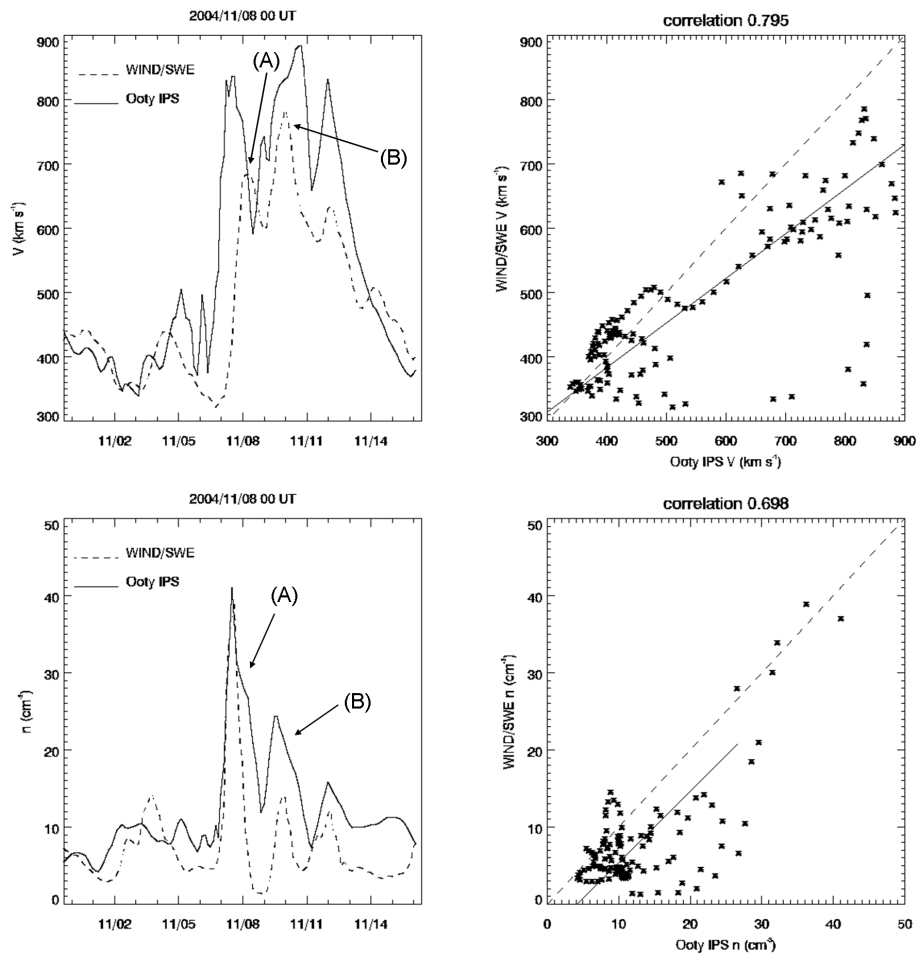


**Fig. 2.** The top-left plot compares the velocity time series at the Wind spacecraft extracted from the Ooty IPS reconstruction (solid line) with Wind solar wind velocity measurements (dashed line), and similarly the bottom-left plot for Wind density measurements. Both the Wind spacecraft velocity and density data are hourly-averaged data that were further averaged with a half-daily cadence to match that of the 3-D reconstruction cadence. The top-right plot shows the correlation of the two data sets for velocity, and similarly the bottom-right plot for density; the dashed line on each correlation plot is for a 100% correlation while the solid line shows the best-fit of the data here. (A) and (B) on the left-hand plots relate to features also highlighted later in Fig. 3 and Fig. 4, with the description of each to be found in the text.

show some of the individual structures of this complex set of events.

The visualisation of these reconstructions allows us to see the individual CMEs as they travel out into the interplanetary medium with the latter catching up to the first. The in-situ comparisons with the reconstructions show as described in the previous section, Fig. 2 (A) relating to Figs. 3 and 4 (i), and Fig. 2 (B) relating to Figs. 3 and 4 (ii) and (iii) at differing times.

High-speed structures engulfing Earth, seen around the same times as the density enhancements, are consistent with the timing and LASCO C2 velocity estimates of the 6 November 2004 Earth-directed events (01:32 UT halo CME and 02:06 UT partial-halo CME) and the 7 November 2004 event. The speed is also consistent with the STELab recon-

structions in Harra et al. (2007). This is also discussed by Bisi et al. (2008a). The other high-speed structure going mainly northward is most likely related to at least one of the many CMEs during this time interval but not necessarily any of the five CMEs discussed here, although increased density is seen going to the North in Fig. 4c and d.

Figure 2 shows the overall increase in both velocity and density associated with these events measured in situ from 7 to 12 November 2004. Individual velocity and density peaks measured by the Wind spacecraft on 7, 10, and 12 November 2004, are matched reasonably well in the 3-D model reconstructions near Earth. There are some differences in the peaks, particularly the timing of the first velocity peak and generally-enhanced reconstructed velocity and density values as compared with those measured by the

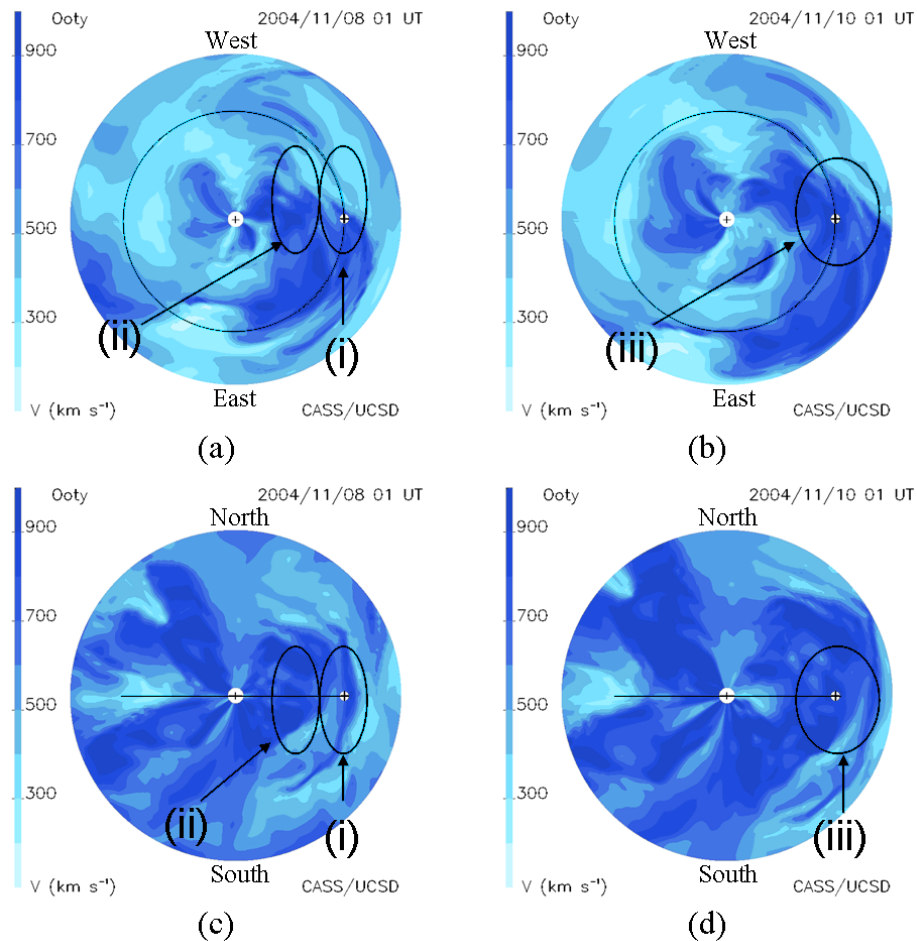


**Fig. 3.** Summary figure of the Ooty ecliptic-, (a) and (b), and meridional-, (c) and (d), cuts through the 3-D velocity reconstruction out to 1.5 AU at the times shown. Various features are circled in the images which are also related to features seen in Fig. 2 as per the text. Material following the circled region (iii) is likely the bottom-right LASCO C2 event in Fig. 1 and not related to the two geomagnetic storms. Earth's orbit is shown as a near-circle or line with the Earth,  $\oplus$ , indicated on each plot. Velocity contours are shown to the left of each of the four images.

Wind spacecraft. A possible and likely explanation for this, particularly for the increased velocity values in general, is that the IPS observations of velocity are higher for the event than those measured in situ further out from the Sun (since the observations of IPS take place between the Sun and the Earth for Earth-directed events). Thus, as the events travel through the interplanetary medium from the Sun towards the Earth (and near-Earth in-situ spacecraft), they decelerate and thus are measured at lower velocities in situ than those reproduced by the kinematic solar wind model. Since no specific deceleration is included in the model (other than when observations show faster velocity running into the back of slower velocity and through the conservation of mass and mass flux as previously mentioned), this is the likely cause of the first peak in the velocity comparison appearing somewhat earlier in the reconstruction than measured in situ (and as shown on the in-situ-comparison plots). Various features

are highlighted in Figs. 3 and 4 and related to the in-situ plots in Fig. 2 as described previously. The various features marked on Figs. 3 and 4 are as follows: region (i) is heliospheric structure associated with the front edge of the interplanetary disturbance which caused the 8 November 2004 geomagnetic storm, most likely caused by a combination of Earth-directed CMEs seen in LASCO on 4 November 2004 at 09:54 UT and 23:30 UT; region (ii) is a combination of the 6 November 2004, 01:32 UT (halo) and 02:06 UT, LASCO C2 CMEs, consistent with the STELab IPS density reconstruction shown in Harra et al. (2007); and region (iii) is the heliospheric structure during the second of the two CDAW storms beginning on 10 November 2004. These are all consistent with the findings of Harra et al. (2007) and Zhang et al. (2007a,b), as well as with Bisi et al. (2008a).

Presently, the University of California, San Diego (UCSD) 3-D reconstructions incorporate a kinematic model.

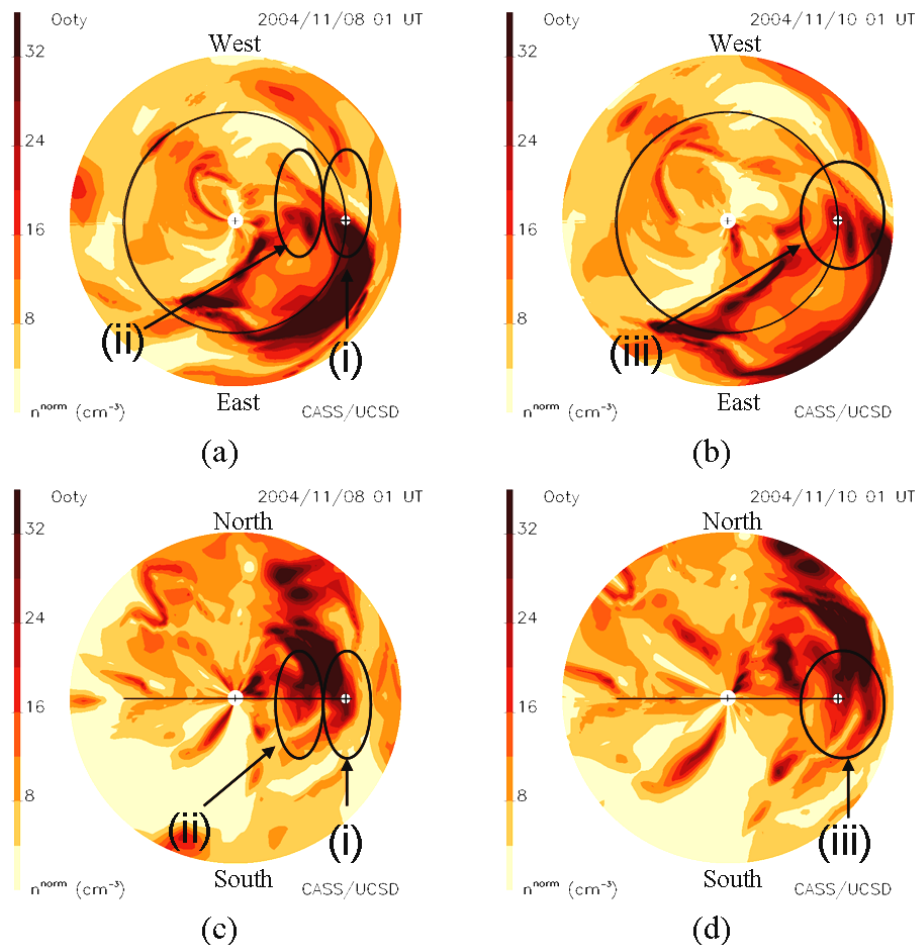


**Fig. 4.** As with Fig. 3 but for density. The expected  $r^{-2}$  density fall-off scaling is used to normalize structures at different radii. Density contours to the left of each image are scaled to 1 AU.

Although individual velocity and density peaks measured by Wind are reproduced in the middle of the Ooty velocity and density reconstructed interval from around 2 November 2004, there is a small enhancement in both parameters in which these peaks reconstruct and do not match quite as well in magnitude as they do with their timing (at least from the comparison with Wind shown here).

Figures 5 and 6 show the weighted sum of LOS crossings during this time interval after projection onto the source surface and at 1 AU respectively of all the Ooty IPS data used for this reconstruction as described in their captions. These figures provide an “error” type analysis first used by Bisi et al. (2009a) to verify the STELab reconstruction of the Whole Heliosphere Interval (WHI). The greater the number of weighted LOS crossings, the higher the confidence in the reconstructions; thus, these plots provide an overall qualitative confidence for the reconstruction in both velocity (top) and  $g$ -level (bottom) projected onto the two heights out from the Sun. These plots show that more information contributes

to reconstructing velocity and density near the ecliptic (since the observations originate from the Earth and thus will naturally have many more LOS crossings near the ecliptic) during this time interval. The number of LOS crossings is not too different when comparing the North to the South up to mid latitudes, but at high latitudes, there appears to be a greater number of LOS crossings suggesting that the distribution of sources may have been slightly greater to the North than to the South. From these observations, the inner heliosphere was successfully reconstructed using the time-dependent 3-D tomography (Figs. 3 and 4). Here, the velocity and density both have the same 3-D-reconstructed resolutions as stated previously.

## 5 Summary and conclusions

The geoeffective storms during November 2004 discussed here and also by Harra et al. (2007); Zhang et al. (2007a,b); Bisi et al. (2007); Bisi et al. (2008b); Bisi et al. (2008a)

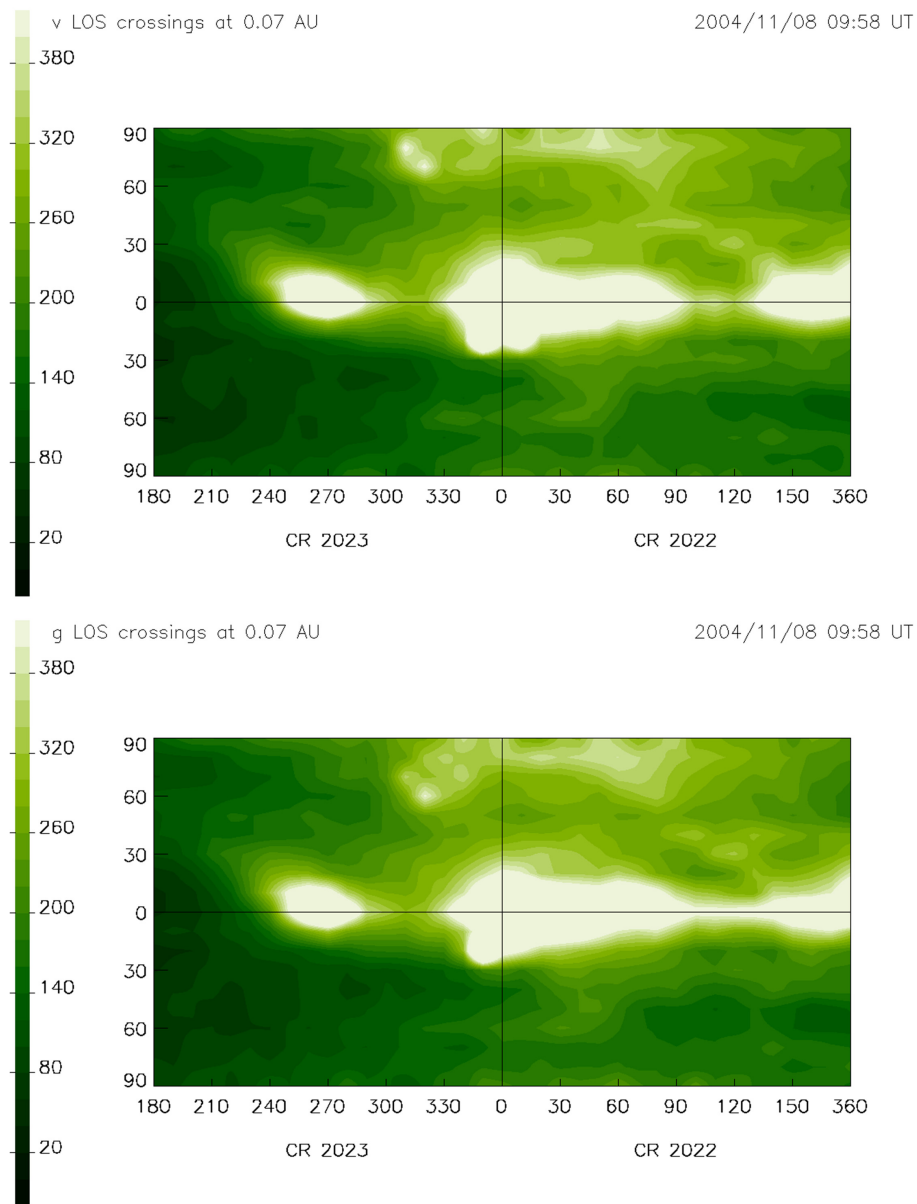


**Fig. 5.** The summed Ooty IPS LOS crossings from velocity (top) and  $g$ -level (bottom) observations (in each  $10^\circ \times 10^\circ$  reconstructed bin) mapped back to the source surface (as per Bisi et al., 2009a). Those portions of these maps having the largest number of LOS crossings have the highest confidence level. The source-surface LOS crossings for each time-reconstructed Carrington map are normalised per day crossings and for the Gaussian temporal and spatial filters. Approximately 32.5 days of observations are used to make the Carrington plots shown here. In the tomography at these Ooty resolutions, the standard deviations of the Gaussian filters are respectively 0.325 day and  $7^\circ$ ; see Jackson et al. (2003) and Jackson et al. (2008) for further details.

and by Bisi et al. (2009b) are well reproduced in velocity and in  $g$ -level-to-density 3-D reconstructions using Ooty IPS data; these are an improvement over previous (Bisi et al., 2007; Bisi et al., 2008b; Bisi et al., 2009b) reconstructions of this interval. The reconstructions are shown to be associated with known in-situ signatures by comparisons with the Wind spacecraft as well as LASCO CME observations and timings (see Harra et al., 2007, for further details).

Overall, the Ooty data reconstruction from the November 2004 complex series of events appears to show improved velocity and density values compared with those using STELab data, which is likely due both to the greater numbers of observed sources and to the increased reconstruction resolution (Bisi et al., 2008a, 2009b). The Ooty reconstructions have twice better the spatial and temporal resolutions compared with those of STELab.

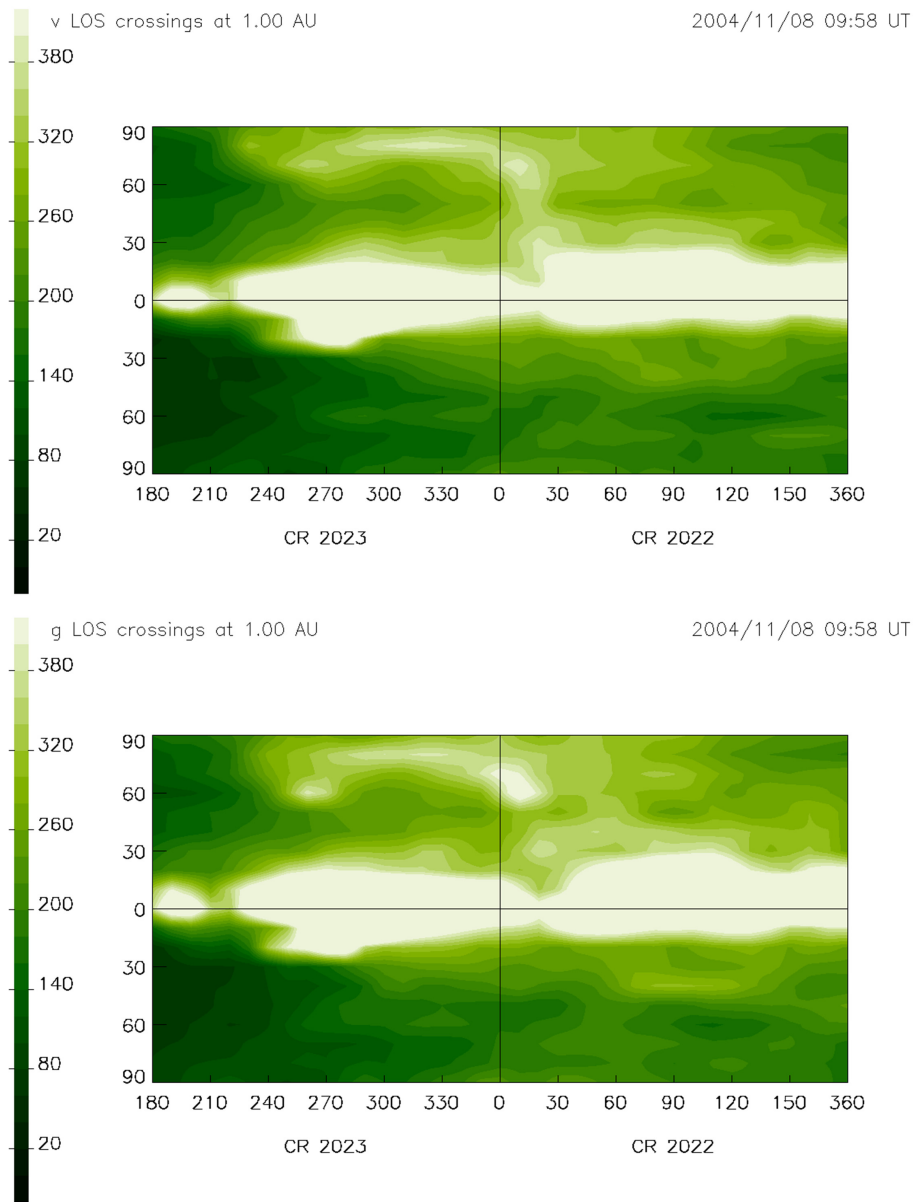


**Fig. 6.** As in Fig. 5 but at a height of 1 AU from the Sun (more pertinent when comparing with  $L_1$ -spacecraft in-situ measurements). As can be seen comparing these with Fig. 5, coverage is greater overall than at the source surface, particularly near the ecliptic.

Our next step is to examine more intervals of complex activity using the Ooty IPS data with the UCSD 3-D-reconstruction tomography and compare these with similar such reconstructions using STELab and SMEI data as well as further comparison with “ground-truth” in-situ measurements.

*Acknowledgements.* The authors (MMB, BVJ, JMC, PPH, and AB) acknowledge AFOSR grant FA9550-06-1-0107, NASA grant NNX08AJ116, and NSF grant ATM0331513, to the University of California, San Diego (UCSD) for support of these 3-D tomographic analyses. The authors wish to thank the Wind|SWE group

for use of the solar wind proton density and velocity measurements used in this paper for in-situ comparisons, as obtained from the World Wide Web. The SOHO|LASCO images and data are courtesy of the LASCO consortium and the SOHO|EIT images are courtesy of the EIT consortium, both via the CDAW WebPages at [http://cdaw.gsfc.nasa.gov/CME\\_list/](http://cdaw.gsfc.nasa.gov/CME_list/).

Topical Editor R. Forsyth thanks A. Gonzalez-Esparza and another anonymous referee for their help in evaluating this paper.

## References

- Bisi, M. M.: Interplanetary Scintillation Studies of the Large-Scale Structure of the Solar Wind, PhD Thesis, The University of Wales, Aberystwyth, 2006.
- Bisi, M. M., Jackson, B. V., Hick, P. P., and Buffington, A.: CME Reconstructions Using Interplanetary Scintillation Data, (invited oral presentation) AOGS 2007 Meeting, 2007.
- Bisi, M. M., Jackson, B. V., Hick, P. P., Buffington, A., Odstrcil, D., and Clover, J. M.: Three-dimensional reconstructions of the early November 2004 Coordinated Data Analysis Workshop geomagnetic storms: Analyses of STELab IPS speed and SMEI density data, *J. Geophys. Res.*, 113, A00A11, doi:10.1029/2008JA013222, 2008a.
- Bisi, M. M., Jackson, B. V., Buffington, A., Hick, P. P., Manoharan, P. K., and Clover, J. M.: Solar Wind and CME Reconstructions in the Inner Heliosphere, (invited oral presentation) AOGS 2008 Meeting, 2008b.
- Bisi, M. M., Jackson, B. V., Buffington, A., Clover, J. M., Hick, P. P., and Tokumaru, M.: Low-Resolution STELab IPS 3D Reconstructions of the Whole Heliosphere Interval and Comparison with in-Ecliptic Solar Wind Measurements from STEREO and Wind Instrumentation, *Solar Phys.*, 256, 201–217, doi:10.1007/s11207-009-9350-9, 2009a.
- Bisi, M. M., Jackson, B. V., Hick, P. P., Buffington, A., and Clover, J. M.: Coronal Mass Ejection Reconstructions from Interplanetary Scintillation Data Using A Kinematic Model: A Brief Review, *Adv. Geosci.*, 14, chapter 12, 2009b.
- Bisi, M. M., Jackson, B. V., Fallows, R. A., Dorrian, G. D., Manoharan, P. K., Clover, J. M., Hick, P. P., Buffington, A., Breen, A. R., and Tokumaru, M.: Solar Wind and CME Studies of the Inner Heliosphere Using IPS Data from STELab, ORT, and EISCAT, *Adv. Geosci.*, in press, 2009c.
- Breen, A. R., Fallows, R. A., Bisi, M. M., Jones, R. A., Jackson, B. V., Kojima, M., Dorrian, G. D., Middleton, H. R., Thomasson, P., and Wannberg, G.: The Solar Eruption of 2005 May 13 and Its Effects: Long-Baseline Interplanetary Scintillation Observations of the Earth-Directed Coronal Mass Ejection, *ApJ Lett.*, 683, L79–L82, doi:10.1086/591520, 2008.
- Brueckner, G. E., Howard, R. A., Koomen, M. J., Korendyke, C. M., Michels, D. J., Moses, J. D., Socker, D. G., Dere, K. P., Lamy, P. L., Llebaria, A., Bout, M. V., Schwenn, R., Simnett, G. M., Bedford, D. K., and Eyles, C. J.: The Large Angle Spectroscopic Coronagraph (LASCO), *Solar Phys.*, 162, 357–402, 1995.
- Burlaga, L. F.: Interplanetary magnetohydrodynamics, New York: Oxford University Press, 1995.
- Delaboudinière, J. P., Artzner, G. E., Brunaud, J., Gabriel, A., Hochedez, J. F., Millier, F., Song, X. Y., Au, B., Dere, K. P., Howard, R. A., Kreplin, R., Michels, D. J., Moses, J. D., Defise, J. M., Jamar, C., Rochus, P., Chauvineau, J. P., Marioge, J. P., Catura, R. C., Lemen, J. R., Shing, L., Stern, R. A., Gurman, J. B., eupert, W. M., Maucherat, A., Clette, F., Cugnon, P., and van Dessel, E. L.: EIT: Extreme-Ultraviolet Imaging Telescope for the SOHO Mission, *Solar Phys.*, 162, 291–312, 1995.
- Domingo, V., Fleck, B., and Poland, A. I.: SOHO: The Solar and Heliospheric Observatory, *Space Sci. Rev.*, 72, 81–84, 1995.
- Harra, L. K., Crooker, N. U., Mandrini, C. H., van Driel-Gesztelyi, L., Dasso, S., Wang, J., Elliott, H., Attrill, G., Jackson, B. V., and Bisi, M. M.: How Does Large Flaring Activity from the Same Active Region Produce Oppositely Directed Magnetic Clouds?, *Solar Phys.*, 244, 95–114, doi:10.1007/s11207-007-9002-x, 2007.
- Hewish, A., Scott, P. F., and Wills, D.: Interplanetary scintillations of small diameter radio sources, *Nature*, 203, 1214–1217, 1964.
- Hick, P. P. and Jackson, B. V.: Heliospheric tomography: an algorithm for the reconstruction of the 3D solar wind from remote sensing observations, in: *Telescopes and Instrumentation for Solar Astrophysics*. Proc. SPIE, edited by: Fineschi, S. and Gumm, M. A., vol. 5171, pp. 287–297, doi:10.1117/12.513122, 2004.
- Jackson, B. V. and Hick, P. P.: Three-dimensional tomography of interplanetary disturbances, in: *Solar and Space Weather Radiophysics: Current status and future developments*, edited by: Gary, D. and Keller, C. U., vol. 314 of *Astrophys. and Space Sci. Lib.*, chap. 17, pp. 355–386, Kluwer Academic Publ., Dordrecht., 2005.
- Jackson, B. V., Hick, P. P., Kojima, M., and Yokobe, A.: Heliospheric tomography using interplanetary scintillation observations, 1. Combined Nagoya and Cambridge data, *J. Geophys. Res.*, 103, 12049–12067, 1998.
- Jackson, B. V., Hick, P. P., Buffington, A., Kojima, M., Tokumaru, M., Fujiki, K., Ohmi, T., and Yamashita, M.: Time-dependent tomography of hemispheric features using interplanetary scintillation (IPS) remote-sensing observations, in: *Solar Wind Ten*, edited by: Velli, M., Bruno, R., Malara, F., and Bucci, B., vol. 679 of *American Institute of Physics Conference Series*, pp. 75–78, doi:10.1063/1.1618545, 2003.
- Jackson, B. V., Bisi, M. M., Hick, P. P., Buffington, A., Clover, J. M., and Sun, W.: Solar Mass Ejection Imager (SMEI) 3D Reconstruction of the 27–28 May 2003 CME Sequence, *J. Geophys. Res.*, 113, A00A15, doi:10.1029/2008JA013224, 2008.
- Jones, R. A., Breen, A. R., Fallows, R. A., Canals, A., Bisi, M. M., and Lawrence, G.: Interaction between coronal mass ejections and the solar wind, *J. Geophys. Res.*, 112, 8107, doi:10.1029/2006JA011875, 2007.
- Kojima, M. and Kakinuma, T.: Solar-cycle dependence of global distribution of solar wind speed, *Space Sci. Rev.*, 53, 173–222, 1990.
- Manoharan, P. K. and Ananthkrishnan, S.: Determination of solar-wind velocities using single-station measurements of interplanetary scintillation, *MNRAS*, 244, 691–695, 1990.
- Manoharan, P. K., Kojima, M., Gopalswamy, N., Kondo, T., and Smith, Z.: Radial Evolution and Turbulence Characteristics of a Coronal Mass Ejection, *ApJ*, 530, 1061–1070, doi:10.1086/308378, 2000.
- Manoharan, P. K., Tokumaru, M., Pick, M., Subramanian, P., Ipavich, F. M., Schenk, K., Kaiser, M. L., Lepping, R. P., and Vourlidas, A.: Coronal Mass Ejection of 2000 July 14 Flare Event: Imaging from Near-Sun to Earth Environment, *ApJ*, 559, 1180–1189, doi:10.1086/322332, 2001.
- McComas, D. J., Bame, S. J., Barker, P., Feldman, W. C., Phillips, J. L., Riley, P., and Griffee, J. W.: Solar Wind Electron Proton Alpha Monitor (SWEPAM) for the Advanced Composition Explorer, *Space Sci. Rev.*, 86, 563–612, doi:10.1023/A:1005040232597, 1998.
- Odstrcil, D. and Pizzo, V. J.: Numerical simulation of interplanetary disturbances, in: *Solspa 2001, Proceedings of the Second Solar Cycle and Space Weather Euroconference*, edited by: Sawaya-Lacoste, H., vol. 477 of *ESA Special Publication*, pp. 281–284,

- 2002.
- Ogilvie, K. W. and Desch, M. D.: The wind spacecraft and its early scientific results, *Adv. Space Res.*, 20, 559–568, 1997.
- Ogilvie, K. W., Chornay, D. J., Fritzenreiter, R. J., Hunsaker, F., Keller, J., Lobell, J., Miller, G., Scudder, J. D., Sittler Jr., E. C., Torbert, R. B., Bodet, D., Needell, G., Lazarus, A. J., Steinberg, J. T., Tappan, J. H., Mavretic, A., and Gergin, E.: SWE, A Comprehensive Plasma Instrument for the Wind Spacecraft, *Space Sci. Rev.*, 71, 55–77, 1995.
- Stone, E. C., Frandsen, A. M., Mewaldt, R. A., Christian, E. R., Margolies, D., Ormes, J. F., and Snow, F.: The Advanced Composition Explorer, *Space Sci. Rev.*, 86, 1–22, doi:10.1023/A:1005082526237, 1998.
- Swarup, G., Sarma, N. V. G., Joshi, M. N., Kapahi, V. K., Bagri, D. S., Damle, S. V., Ananthkrishnan, S., Balasubramanian, V., Bhave, and Sinha, R. P. P.: Large Steerable Radio Telescope at Ootacamund, India, *Nature*, 230, 185–188, 1971.
- Zhang, J., Richardson, I. G., Webb, D. F., Gopalswamy, N., Huttunen, E., Kasper, J. C., Nitta, N. V., Poomvises, W., Thompson, B. J., Wu, C.-C., Yashiro, S., and Zhukov, A. N.: Solar and interplanetary sources of major geomagnetic storms ( $D_{st} \leq -100$  nT) during 1996–2005, *J. Geophys. Res.*, 112, 10102, doi:10.1029/2007JA012321, 2007a.
- Zhang, J., Richardson, I. G., Webb, D. F., Gopalswamy, N., Huttunen, E., Kasper, J. C., Nitta, N. V., Poomvises, W., Thompson, B. J., Wu, C.-C., Yashiro, S., and Zhukov, A. N.: Correction to “Solar and interplanetary sources of major geomagnetic storms ( $D_{st} \leq -100$  nT) during 1996–2005”, *J. Geophys. Res.*, 112, 12103, doi:10.1029/2007JA012891, 2007b.